SPACE SCIENCES

Micrometeoroid infall onto Saturn's rings constrains their age to no more than a few hundred million years

Sascha Kempf[1,2]*, Nicolas Altobelli[3], Jürgen Schmidt[4,5], Jeffrey N. Cuzzi[6], Paul R. Estrada[6], Ralf Srama[7]

There is ongoing debate as to whether Saturn's main rings are relatively young or ancient— having been formed shortly after Saturn or during the Late Heavy Bombardment. The rings are mostly water-ice but are polluted by non-icy material with a volume fraction ranging from ~0.1 to 2%. Continuous bombardment by micrometeoroids exogenic to the Saturnian system is a source of this non-icy material. Knowledge of the incoming mass flux of these pollutants allows estimation of the rings' exposure time, providing a limit on their age. Here we report the final measurements by Cassini's Cosmic Dust Analyzer of the micrometeoroid flux into the Saturnian system. Several populations are present, but the flux is dominated by low-relative velocity objects such as from the Kuiper belt. We find a mass flux between $6.9 \cdot 10^{-17}$ and $2.7 \cdot 10^{-16}$ kg m^{-2}s^{-1} from which we infer a ring exposure time $\lesssim$100 to 400 million years in support of recent ring formation scenarios.

INTRODUCTION

The Saturnian rings are the brightest of the four ring systems of the solar system owing to their nearly pristine water-ice composition (>95% by mass) and are easily the heaviest having a total mass a little less than half the mass of the moon Mimas (1, 2). Because the ring mass covers a surface area 10^4 to 10^5 times greater than a moon of equal mass, the rings are extremely susceptible to bombardment by micrometeoroids exogenic to the Saturnian system, which deliver impurities and gradually darken initially bright icy rings over time. The resulting ring color and albedo variations with radial distance from Saturn provide a key for constraining the ring age (3, 4).

The rate at which exogenic micrometeoroids affect the rings at some location can be expressed in terms of a direct deposition time t_{dd} here normalized to a ring radius $r_0 = 1.8 R_S$ (Saturn's radius, $R_S = 60{,}268$ km). If no exogenic material is lost during an impact, t_{dd} can be written in terms of the impact flux $\dot{\sigma}_{im}$ as (3)

$$t_{dd} = \sigma_0/\dot{\sigma}_{im} \simeq \sigma_0/2 f_g F_\infty \qquad (1)$$

where σ_0 is the ring's surface mass density at r_0, F_∞ is the one-sided, interplanetary mass flux (kg m^{-2}s^{-1}) into the Saturnian system, unaffected by Saturn's gravity, and f_g is the enhancement of F_∞ due to gravitational focusing by Saturn at the ring location (3, 4). Equation 1 is essentially the time it takes a ring annulus to be impacted by its own mass. Knowledge of F_∞ and of f_g allows us to obtain an upper bound on the pollution time scale for the rings, assuming they start as pure ice and darken to their current state.

RESULTS

Here, we report the mass flux F_∞ derived from measurements by the charge-sensitive entrance grid system (5) (QP) of the Cosmic Dust Analyzer (6) (CDA) on the Cassini spacecraft, which began orbiting Saturn in July 2004 until end of mission in September 2017. The QP sensor measures the charge signature induced onto an entrance grid system when a grain enters CDA from which information on the particle's velocity and size are derived, within an accuracy of a few percent (see Fig. 1 and text S1) (5). Each QP signature yields up to four solutions for the velocity vector, from which we backtrack the corresponding trajectory in time. Velocity vector solutions that result in trajectories crossing Saturn's Hill sphere (characterized by Saturn's Hill radius, $R_H = 1100 R_S$) imply an exogenic origin (see text S2).

We derive the grain radius a_d from the dust charge $Q_d = 4\pi\epsilon_0 a_d \phi_d$ measured by QP (7), where the electrostatic equilibrium potential ϕ_d is approximately +5 V for particles exposed to the solar wind and solar ultraviolet (UV) (8). Because of the rather small sensitive area of in situ dust sensors, detections of interplanetary or interstellar dust (ISD) particles are rare events. When Cassini is within Saturn's diffuse E ring, where the dust flux is dominated by submicrometer water ice grains (9), it is hard to identify exogenic dust unambiguously. To exclude observational biases, we restricted our analysis to 163 QP events recorded after Cassini's arrival at Saturn outside of the dust-rich E ring region extending radially to Titan's orbit (~20 R_S) and vertically about ±1 R_S around Saturn's equatorial plane (fig. S5). Charged dust grains can only be detected by the QP sensor during periods when the grid system is not exposed to solar UV. We identified 73 particles being certainly exogenic because all possible velocity vectors support trajectories unbound to Saturn. An additional 90 particles, with at least one Saturn-unbound trajectory solution with low injection speed at R_H and highly eccentric Saturn-bound trajectory solutions, are considered as possibly exogenic. For all exogenic trajectory solutions of each particle, we derive the injection speed relative to Saturn at R_H (Fig. 2) and the heliocentric orbital elements (figs. S2 and S3). The heliocentric orbital elements provide a constraint on the particles' origin, while the injection

[1]Department of Physics, University of Colorado, Boulder, CO 80309, USA. [2]Laboratory for Atmospheric and Space Physics, University of Colorado, Boulder, CO 80303, USA. [3]ESA-ESAC, E-28691 Villanueva de la Cañada, Madrid, Spain. [4]Institut für Geologische Wissenschaften, Freie Universität Berlin, Berlin, Germany. [5]Space Physics and Astronomy Research Unit, University of Oulu, Oulu, Finland. [6]Space Science Division, NASA Ames Research Center, Moffett Field, CA 94035, USA. [7]Institut für Raumfahrtsysteme, Universität Stuttgart, Stuttgart, Germany.
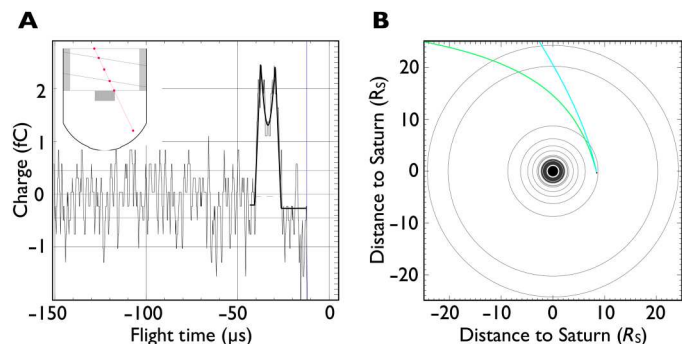*Corresponding author. Email: sascha.kempf@colorado.edu

Fig. 1. QP detection of an IDP on 2008-260/13:21:22 UTC at a distance of 13.0 R_S to Saturn. (**A**) Its charge of $Q_d = 2.7$ fC (relative to the negative baseline around -20 µs) corresponds to a grain radius of 4.8 µm. The inset shows the particle's trajectory in the CDA reference frame reconstructed from its QP signature. (**B**) The trapezoidal feature in (A) with a central dip corresponds to two possible particle orbits, both are trajectories of interplanetary grains in prograde orbits (blue, $a = 9.5$ atronomical units (AU), $e = 0.26$, $i = 13.1°$; green, $a = 13.6$ AU, $e = 0.39$, $i = 17.9°$). Circles denote the orbital distances of Saturnian satellites as well as the ring system and the planet.

velocity at the Hill sphere is used to derive the gravitational focusing factor f_g. Further details are provided in texts S2 and S3.

The certainly exogenic particle set contains both sun-bound and sun-unbound orbits, suggesting a combination of various dynamical dust populations. We call the sun-bound exogenic material sun-bound interplanetary dust particles (IDPs). We argue that the possibly exogenic particles are indeed also probably exogenic and actually sun-bound IDPs because their nominally Saturn-bound orbits are highly eccentric, which otherwise could imply a flux from ongoing collisional grinding of Saturn's irregular satellite population (10). Their flux is comparable to the certainly exogenic IDP flux itself, which is unlikely for inward-evolving particles from the irregulars because Iapetus and Titan are expected to sweep up most of those grains (see Materials and Methods) (11). Moreover, small errors in the trajectories of these low relative velocity objects can nudge the trajectory solutions from bound to unbound. Whether this group is interplanetary or sourced from the irregular satellites, the orbital characteristics of these particles imply that they will eventually hit the rings at high speeds, contributing to the

impact flux and playing a role in the rings' compositional evolution and exposure age.

The sun-bound IDPs have low to moderate heliocentric inclinations, as expected for grains generated by Edgeworth-Kuiper belt (EKB) object or Jupiter Family comet (JFC) sources (12–14) and have a pronounced modal injection speed at R_H of 4.3 km s^{-1} (obtained from a fit to the histogram shown in Fig. 2). Their radii have an upper limit of about 60 µm, if one excludes a single huge outlier (250-µm radius; see texts S2, S5, and S6). This upper size limit is statistically significant and appears to be in agreement with the maximum grain size expected from the ISD-EKBs collision process, dominating dust production in the contemporary EKB (15). Evidence for EKB dust even reaching the Earth distance was recently inferred from exposure ages of IDPs collected in Earth's atmosphere (16).

Certainly exogenic particles with sun-unbound trajectory solutions appear to contain a small contribution with the typical ISD signature (17), but most of them have a signature distinct from the ISD. A detailed understanding of the origin of those particles being beyond the scope of this paper, we simply refer to this population hereafter as sun-unbound IDPs, because it is not uncommon for dust grains originating from solar system objects to end up on sun-unbound trajectories (18).

The typical injection speeds of the sun-bound IDPs, either separating or combining the certainly exogenic and the probably exogenic populations (Fig. 2), are considerably lower than the previously used 14.4 km s^{-1}, which was based on the assumption that dust populating the outer solar system was dominantly on highly eccentric and inclined Oort cloud–like orbits, which had implied a gravitational focusing flux enhancement factor of $f_g \sim 3$ at the location of the main rings (1.8 R_S)(3, 19). Our lower injection speed results in a more pronounced effect of gravitational focusing at the ring location, (text S3), with a flux enhancement by at least a factor of $f_g \sim 30$. In calculating F_∞ from measured particle counts and radii, the particle masses used assume a mixture of silicates, organics, and ices having a mean density of $\rho_d = 2,800$ kg m^{-3} (text S6) (20).
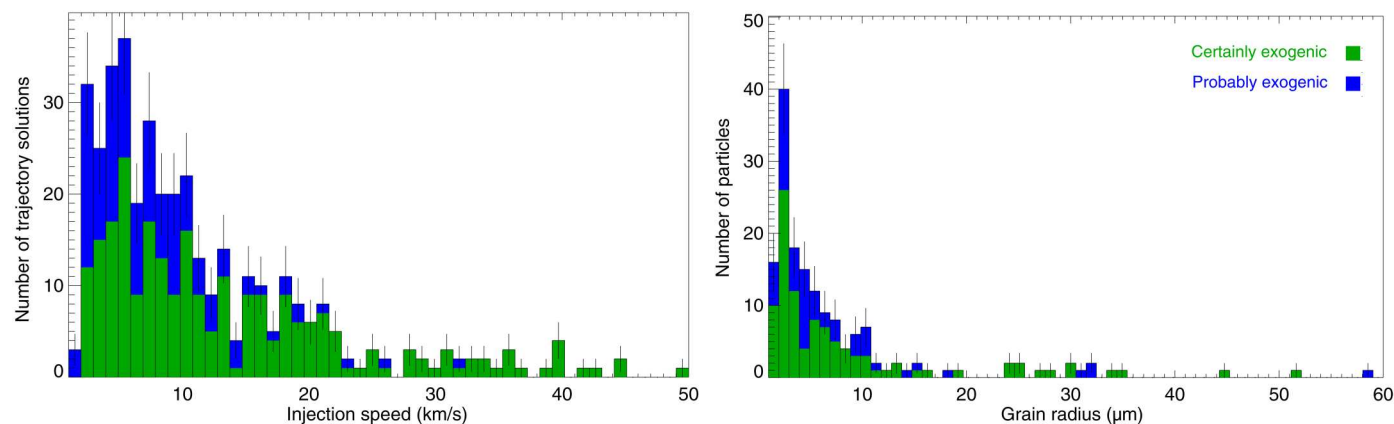
Fig. 2. Speed distribution of the dust particles. Left: Distribution of injection speeds computed at Saturn's Hill radius for all particles with at least one exogenic solution. The fraction of detections for which all solutions are exogenic is shown in green. **Right:** Size distribution of grains with at least one exogenic solution (see also text S5).

DISCUSSION

The uncertainty in the origin of the grains dominates all other uncertainties. If we consider only the grains classified as certainly exogenic, then we find a lower bound to the mass flux of $F_\infty \simeq 6.9 \cdot 10^{-17}$ kg m^{-2}s^{-1} (see text S4). Including both the certainly and probably exogenic grains (but still excluding the 250-μm grain) then provides the most likely estimate for the mass flux of $F_\infty \simeq 2.7 \cdot 10^{-16}$ kg m^{-2}s^{-1} (text S4).

Using the total value for F_∞, we estimate the time, t_{pol}, it would take for a pure ice ring at 1.8 R_S to be polluted to its current state, adopting a midrange value for the observed non-icy volume fraction of $\upsilon \sim 0.3\%$ (21), and a surface mass density of $\sigma_0 \sim 520$ kg m^{-2} in the B ring, consistent with recent Cassini measurements for the ring mass (2). For a time-independent flux, the mass flux per unit area at which material hits the ring is $\dot{\sigma}_{im}$ (Eq. 1), so the exposure time to accumulate the observed pollutant volume fraction υ is (see Materials and Methods)

$$
t_{pol} \sim 100 \text{ Ma} \left(\frac{\sigma_0}{520 \text{ kg m}^{-2}} \right) \left(\frac{2.7 \cdot 10^{-16} \text{ kg m}^{-2} \text{ s}^{-1}}{F_\infty} \right) \left(\frac{2800 \text{ kg m}^{-3}}{\rho_d} \right) \left(\frac{30}{f_g} \right) \left(\frac{0.1}{\eta} \right) \tag{2}
$$

If the probably exogenic detections are not included in the computation of F_∞, then the exposure age would increase by a factor of 4 or ~400 million years (Ma). In Eq. 2, although the entire mass of the affecting flux is deposited in the rings, we have assumed that only a fraction $\eta = 10\%$ of a micrometeoroid retains its absorbing properties after impact and contributes as pollutant. Such low values have been adopted in previous models that assumed that the micrometeoroids are considerably icy (3), so the estimate may be quite conservative. Increasing η would lower these exposure ages.

We find that the ring exposure age for the current mass influx into the Saturnian system does not allow the rings to be formed together with Saturn and its satellites (22, 23) nor slightly later during the Late Heavy Bombardment (24). Saturn's current rings cannot be primordial. An initially massive primordial ring has been posited to better resist the effects of pollution as it viscously evolves to its current state over billions of years (25). However, viscous evolution of such a massive ring occurs quickly, so that the ring spends the vast majority of its lifetime near its current mass (25) and would absorb a much higher-than-observed volume fraction of pollutants during that time. Moreover, the IDP flux at Saturn F_∞ might well not have been constant throughout the solar system's history: It was probably larger in the early days (26, 27), further complicating such an old-ring scenario.

MATERIALS AND METHODS
Magnitude of the micrometeoroid flux

CDA's grain detections that correspond to probably exogenic have both interplanetary (unbound with respect to Saturn) and bound orbital solutions, which arise because of the ambiguity in determining the x component of the grain's velocity (see text S1). For this subset, the unbound solutions for the grains correspond to injection velocities into the Hill sphere that are mainly concentrated at lower speeds than our modal value (see fig. S4), whereas their bound

solutions have average $e > 0.5$. If the circumplanetary solution is the correct one, then some discussion as to the origin of these grains is in order with Saturn's irregular moons such as Phoebe seeming the most likely source. Micrometer- to tens-of-micrometer–sized grains ejected from the irregular satellites would evolve inward due to Poynting-Robertson drag. However, the largest grains have a probability near unity of impacting Iapetus, while grains $\lesssim 5$ μm are not likely to get past Titan; on the other hand, grains <5 μm develop progressively higher e and can be lost to Saturn and its rings relatively quickly (11).

Of the grains that also have bound solutions, most were detected inside Titan's orbit, and of these, slightly less than half are >5 μm. This represents a sizable fraction of the total flux. It has been estimated that a few Mimas masses of collisionally produced material from Saturn's irregular satellites was generated over the age of the Solar System but that most of this material would have been produced in the first few 100 Ma after Saturn's formation (10). However, the frequency of detections as captured by CDA would argue against this, if they are indeed products of the irregulars, and suggest that collisional grinding is an ongoing process (11), as perhaps evidenced by Phoebe's dust ring (28). A relatively constant rate of production would produce a flux comparable to what is observed. Moreover, such a process might lead to a "jump" in the flux as may be measured from outside the Hill sphere to within. Measurements and models of the micrometeoroid flux between the planets include multiple populations (14), including JFCs (of which the 250-μm grain may be one), but collisionally ground irregular satellite material could then be another source within the circumplanetary environment. For the purposes of ring pollution and evolution, however, it actually does not matter which is the case. The orbital characteristics of these grains imply that they will eventually hit the rings at hypervelocities and contribute to the impact flux $\dot{\sigma}_{im}$, and thus, it is most appropriate to include them in the estimate of ring age. Given these uncertainties, we favor an exogenic origin so that our nominal value for F_∞ should include all particle detections flagged as either certainly exogenic or probably exogenic. While we have excluded the single detection of a very large IDP grain (size >250 μm) for statistical robustness in the mass flux computation, the extremely low densities of such particles (see text S6) make their mass comparable to those of 10 times smaller grains. We are therefore confident that the bulk of the mass flux is deposited by the particle populations sampled by CDA with sufficient statistics over the mission duration (see text S5).

Estimates for the ring age and sources of uncertainty therein

The rate per unit area at which micrometeoroids hit the rings is given by the impact flux $\dot{\sigma}_{im}$ (Eq. 1). This impact flux depends also on a probability of impact as the micrometeoroid crosses the ring plane, which is a function of the rings' local optical depth (3, 4). For the B ring where optical depths >1, this probability is effectively unity, so that $\dot{\sigma}_{im} \simeq 2F_\infty f_g$ is a reasonable estimate there. The accumulated mass density of pollutant in time t_{pol} is $\sigma_{pol} \simeq \eta \dot{\sigma}_{im} t_{pol}$, where the factor $\eta \leq 1$ allows for the possibility that a fraction of the impactor's optically absorbing material is transformed by evaporation and recondensation into nonabsorbing material and thus does not contribute to darkening the rings (3). The mass fraction of pollutant after this time is then $\sigma_{pol}/(\sigma_{pol} +$

$\sigma_0) \simeq \sigma_{pol}/\sigma_0$, for $\sigma_{pol} \ll \sigma_0$. Converting from mass fraction to volume fraction for a ring particle is done by multiplying by the ratio of mean ring particle density to the density of the pollutant material $\rho_{pol} = 2.8 \cdot 10^3$ kg/m^3 within the ring particle, $\upsilon \simeq (\rho/\rho_{pol})(\sigma_{pol}/\sigma_0)$, where $\rho = \rho_{pol}\upsilon + \rho_{ice}(1 - \upsilon)$, $\rho_{ice} = 0.9 \cdot 10^3$ kg/m^3 is the density of ice and $\upsilon \ll 1$. Noting the accumulated mass fraction is just the ratio of the exposure time to the direct deposition time, the time to accumulate the observed volume fraction υ assuming none of the impacting material is lost is

$$t_{\text{pol}} \simeq \frac{\rho_{pol}}{\rho} \, \upsilon \frac{t_{\text{dd}}}{\eta} = \frac{\rho_{pol}}{\rho} \, \upsilon \, \frac{\sigma_0}{2F_\infty f_g \eta} \qquad (3)$$

which is used to give the estimate of $\sim$100 Ma in Eq. 2, where the value of $f_g = 30$ is derived from the modal value of the injection velocity distribution at Saturn Hill's sphere of 4.3 km s^{-1} (see Fig. 2).

All of the mass of an impactor is deposited in the rings, but the fraction of a micrometeoroid's pollutant that survives a hyper-velocity impact with a ring particle as absorbing material most likely depends on the compositional make-up of the incoming projectile. Unfortunately, impacting carbonaceous material into porous ice targets at impact speeds expected at the rings remains unaddressed experimentally. Several past papers modeling ring pollution have discussed this parameter (3, 29) and do provide certain constraints on the value of η. Doyle et al. (29) assume a value of $\eta \sim 0.1$ relative to the total impactor mass, citing the persistence of a certain number of carbon-carbon bonds from particles observed by the Vega spacecraft with impact speeds of 70 km s^{-1} (30). Moreover, previous models of micrometeoroid bombardment and ballistic transport of impact ejecta have assumed that the exogenic projectiles were Oort cloud material that had a substantial volatile fraction that would vaporize on impact, so that only a fraction $\eta \sim 0.05$ of the material, non-icy and presumably carbonaceous, would survive in its absorbing form (3, 31). Cuzzi and Estrada (3) showed with their compositional evolution models (discussed in detail in their section 4.3) that the shape of the radial profile of ring color about the B ring–C ring boundary is directly tied to the local abundance of pollutant, which placed further constraints on η. Smaller values of η were not considered reasonable since it would not be possible to simultaneously explain the contrast in darkening between low and high optical depth regions and the gradual color transition that arises as a result of ballistic transport of both intrinsic and exogenic material across the C ring and inner B ring (3). This is because ballistic transport homogenizes composition when allowed to act over very long time scales (31), so the fact that a contrast still exists implies that ballistic transport has not acted for that long. Here, we adopt a nominal $\eta \sim 0.1$ for grains with no substantial volatile fraction, remaining consistent with the modeling constraints of (3, 29).

It should be pointed out that the value of the volume fraction υ depends on the model used for the ring particles. Like (3), we assume an intramixing model in which the non-icy constituents are small inclusions volumetrically mixed within an ice matrix. This gives the minimum υ. Probably the most complete analyses of visual wavelength data in terms of actual composition have been conducted by (32, 33). Cuzzi et al. (32) use intramixing models that uniquely account for rough particles with on-surface shadowing that, if not allowed, can reduce particle albedo and bias the fractional pollutant toward unrealistically high values.

They derive values for υ of a fraction of a percent in the A and B rings and up to several percent in the C ring. On the other hand, (33) obtained much larger υ because, in addition to not allowing for the complications of on-particle shadowing, they assume an intimate "salt and pepper" regolith mixing model with larger "pollutant" grains relative to the tiny inclusions assumed in (32). However, there are several arguments as to why the intramix model is the more likely one. First, it was found that it is not possible to sufficiently color the rings to their observed redness unless the absorbing material was "intramixed" into the ring particles volumetrically (3). Second, the derived values for υ in (32) are in agreement with those derived from centimeter-wavelength radiometry by the Cassini RADAR (21) where, at these long wavelengths, any plausible granular intimate mixture behaves like an intramixture, so the good agreement between Cassini radiometry and (32) supports the assumptions of the latter. Last, micrometeoroid impacts would likely shatter the material into smaller inclusions, and the measurements of the flux of material falling into Saturn from the rings during the Cassini Grand Finale were characterized by a distribution of nanograins (34–36).

Using the values for ρ_d and η as discussed above, we calculate the upper bound on the exposure time for the B ring where a majority of the ring mass resides using an average value for the volume fraction there of $\upsilon = 0.003$ as determined in (21). Our adopted average surface density $\sigma_0 = 520$ kg m^{-2} is obtained from the mass estimate of the B ring of $\sim$0.23 Mimas masses (2) spread over the radial extent of the B ring from 92,000 to 117,580 km. We consider this a reasonably solid upper bound because we have made the extreme assumption that the rings began as pure water ice, which is almost certainly not true. Other factors that would lower the exposure age would be a higher flux in the past and a larger η. Factors that would increase the exposure age would be if impactors have considerable porosity or if the flux has been intermittent over the rings' lifetime. The former would likely only add at most a factor of 2, whereas for the latter, observed structures in the rings attributed to micrometeoroid bombardment and ballistic transport like the inner B ring edge require a persistent flux to sculpt and maintain (31).

Supplementary Materials

This PDF file includes:
Supplementary Texts S1 to S6
Figs. S1 to S13
Tables S1 and S2
References

REFERENCES AND NOTES

1. L. W. Esposito, M. O'callaghan, R. A. West, The structure of Saturn's rings–Implications from the Voyager stellar occultation. *Icarus* **56**, 439–452 (1983).
2. L. Iess, B. Militzer, Y. Kaspi, P. Nicholson, D. Durante, P. Racioppa, A. Anabtawi, E. Galanti, W. Hubbard, M. J. Mariani, P. Tortora, S. Wahl, M. Zannoni, Measurement and implications of Saturn's gravity field and ring mass. *Science* **364**, eaat2965 (2019).
3. J. N. Cuzzi, P. R. Estrada, Compositional evolution of saturn's rings due to meteoroid bombardment. *Icarus* **132**, 1–35 (1998).
4. R. H. Durisen, P. W. Bode, J. N. Cuzzi, S. E. Cederbloom, B. W. Murphy, Ballistic transport in planetary ring systems due to particle erosion mechanisms: II. Theoretical models for Saturn's A- and B-ring inner edges. *Icarus* **100**, 364–393 (1992).
5. S. Auer, E. Grün, R. Srama, S. Kempf, R. Auer, The charge and velocity detector of the cosmic dust analyzer on Cassini. *Planet. Space Sci.* **50**, 773–779 (2002).

6. R. Srama, T. J. Ahrens, N. Altobelli, S. Auer, J. G. Bradley, M. Burton, V. V. Dikarev, T. Economou, H. Fechtig, M. Görlich, M. Grande, A. Graps, E. Grün, O. Havnes, S. Helfert, M. Horanyi, E. Igenbergs, E. K. Jessberger, T. V. Johnson, S. Kempf, A. V. Krivov, H. Krüger, A. Mocker-Ahlreep, G. Moragas-Klostermeyer, P. Lamy, M. Landgraf, D. Linkert, G. Linkert, F. Lura, J. A. M. McDonnell, D. Möhlmann, G. E. Morfill, M. Müller, M. Roy, G. Schäfer, G. Schlotzhauer, G. H. Schwehm, F. Spahn, M. Stübig, J. Svestka, V. Tschernjawski, A. J. Tuzzolino, R. Wäsch, H. A. Zook, The cassini cosmic dust analyzer. *Space Sci. Rev.* **114**, 465–518 (2004).

7. S. Kempf, R. Srama, N. Altobelli, S. Auer, V. Tschernjawski, J. Bradley, M. E. Burton, S. Helfert, T. V. Johnson, H. Krüger, G. Moragas-Klostermeyer, E. Grün, Cassini between Earth and asteroid belt: First in-situ charge measurements of interplanetary grains. *Icarus* **171**, 317–335 (2004).

8. M. Horányi, Charged dust dynamics in the solar system. *Annu. Rev. Astron. Astrophys.* **34**, 383–418 (1996).

9. S. Kempf, U. Beckmann, G. Moragas-Klostermeyer, F. Postberg, R. Srama, T. Economou, J. Schmidt, F. Spahn, E. Grün, The E ring in the vicinity of Enceladus: I. Spatial distribution and properties of the ring particles. *Icarus* **193**, 420–437 (2008).

10. W. F. Bottke, D. Nesvorný, D. Vokrouhlický, A. Morbidelli, The irregular satellites: The most collisionally evolved populations in the solar system. *Astron. J.* **139**, 994–1014 (2010).

11. D. Tamayo, J. A. Burns, D. P. Hamilton, M. M. Hedman, Finding the trigger to Iapetus' odd global albedo pattern: Dynamics of dust from Saturn's irregular satellites. *Icarus* **215**, 260–278 (2011).

12. A. R. Poppe, M. Horányi, On the Edgeworth-Kuiper belt dust flux to Saturn. *Geophys. Res. Lett.* **39**, L15104 (2012).

13. A. R. Poppe, An improved model for interplanetary dust fluxes in the outer Solar System. *Icarus* **264**, 369–386 (2016).

14. A. R. Poppe, C. M. Lisse, M. Piquette, M. Zemcov, M. Horányi, D. James, J. R. Szalay, E. Bernardoni, S. A. Stern, Constraining the solar system's debris disk with in situ *new horizons* measurements from the Edgeworth–Kuiper belt. *Astrophys. J. Lett.* **881**, L12 (2019).

15. S. Yamamoto, T. Mukai, Dust production by impacts of interstellar dust on Edgeworth-Kuiper belt objects. *Astron. Astrophys.* **329**, 785–791 (1998).

16. L. P. Keller, G. J. Flynn, Evidence for a significant Kuiper belt dust contribution to the zodiacal cloud. *Nat. Astron.* **6**, 731–735 (2022).

17. N. Altobelli, F. Postberg, K. Fiege, M. Trieloff, H. Kimura, V. J. Sterken, H. W. Hsu, J. Hillier, N. Khawaja, G. Moragas-Klostermeyer, J. Blum, M. Burton, R. Srama, S. Kempf, E. Grün, Flux and composition of interstellar dust at Saturn from Cassini's Cosmic Dust analyzer. *Science* **352**, 312–318 (2016).

18. A. Wehry, I. Mann, Identification of β-meteoroids from measurements of the dust detector onboard the Ulysses spacecraft. *Astron. Astrophys.* **341**, 296–303 (1999).

19. D. H. Humes, Results of Pioneer 10 and 11 meteoroid experiments: Interplanetary and near-Saturn. *J. Geophys. Res.* **85**, 5841–5852 (1980).

20. D. H. Wooden, H. A. Ishii, M. E. Zolensky, Cometary dust: The diversity of primitive refractory grains. *Phil. Trans. R. Soc. A* **375**, 20160260 (2017).

21. Z. Zhang, A. G. Hayes, M. A. Janssen, P. D. Nicholson, J. N. Cuzzi, I. de Pater, D. E. Dunn, Exposure age of Saturn's A and B rings, and the Cassini division as suggested by their non-icy material content. *Icarus* **294**, 14–42 (2017).

22. R. M. Canup, Origin of Saturn's rings and inner moons by mass removal from a lost Titan-sized satellite. *Nature* **468**, 943–946 (2010).

23. A. Crida, S. Charnoz, Formation of regular satellites from ancient massive rings in the solar system. *Science* **338**, 1196–1199 (2012).

24. S. Charnoz, A. Morbidelli, L. Dones, J. Salmon, Did Saturn's rings form during the late heavy bombardment? *Icarus* **199**, 413–428 (2009).

25. J. Salmon, S. Charnoz, A. Crida, A. Brahic, Long-term and large-scale viscous evolution of dense planetary rings. *Icarus* **209**, 771–785 (2010).

26. K. Zahnle, P. Schenk, H. Levison, L. Dones, Cratering rates in the outer solar system. *Icarus* **163**, 263–289 (2003).

27. S. Charnoz, L. Dones, L. W. Esposito, P. R. Estrada, M. M. Hedman, Saturn After Cassini-Huygen, Saturn from Cassini-Huygens, in *Origin and Evolution of Saturn's Ring System*, M. K. Dougherty, L. W. Esposito, S. M. Krimigis, Eds. (Springer, 2009), p. 537–575.

28. A. J. Verbiscer, M. F. Skrutskie, D. P. Hamilton, Saturn's largest ring. *Nature* **461**, 1098–1100 (2009).

29. L. R. Doyle, L. Dones, J. N. Cuzzi, Radiative transfer modeling of Saturn's outer B ring. *Icarus* **80**, 104–135 (1989).

30. J. Kissel, F. R. Krueger, Ion formation by impact of fast dust particles and comparison with related techniques. *Appl. Phys. A* **42**, 69–85 (1987).

31. P. R. Estrada, R. H. Durisen, J. N. Cuzzi, D. A. Morgan, Combined structural and compositional evolution of planetary rings due to micrometeoroid impacts and ballistic transport. *Icarus* **252**, 415–439 (2015).

32. J. N. Cuzzi, R. G. French, A. R. Hendrix, D. M. Olson, T. Roush, S. Vahidinia, HST-STIS spectra and the redness of Saturn's rings. *Icarus* **309**, 363–388 (2018).

33. M. Ciarniello, G. Filacchione, E. D'Aversa, F. Capaccioni, P. D. Nicholson, J. N. Cuzzi, R. N. Clark, M. M. Hedman, C. M. D. Ore, P. Cerroni, C. Plainaki, L. J. Spilker, Cassini-VIMS observations of Saturn's main rings: II. A spectrophotometric study by means of Monte Carlo ray-tracing and Hapke's theory. *Icarus* **317**, 242–265 (2019).

34. J. H. Waite Jr., R. S. Perryman, M. E. Perry, K. E. Miller, J. Bell, T. E. Cravens, C. R. Glein, J. Grimes, M. Hedman, J. Cuzzi, T. Brockwell, B. Teolis, L. Moore, D. G. Mitchell, A. Persoon, W. S. Kurth, J.-E. Wahlund, M. Morooka, L. Z. Hadid, S. Chocron, J. Walker, A. Nagy, R. Yelle, S. Ledvina, R. Johnson, W. Tseng, O. J. Tucker, W.-H. Ip, Chemical interactions between Saturn's atmosphere and its rings. *Science* **362**, eaat2382 (2018).

35. H.-W. Hsu, J. Schmidt, S. Kempf, F. Postberg, G. Moragas-Klostermeyer, M. Seiß, H. Hoffmann, M. Burton, S. Ye, W. S. Kurth, M. Horányi, N. Khawaja, F. Spahn, D. Schirdewahn, J. O'Donoghue, L. Moore, J. Cuzzi, G. H. Jones, R. Srama, In situ collection of dust grains falling from Saturn's rings into its atmosphere. *Science* **362**, eaat3185 (2018).

36. D. G. Mitchell, M. E. Perry, D. C. Hamilton, J. H. Westlake, P. Kollmann, H. T. Smith, J. F. Carbary, J. H. Waite, R. Perryman, H.-W. Hsu, J.-E. Wahlund, M. W. Morooka, L. Z. Hadid, A. M. Persoon, W. S. Kurth, Dust grains fall from Saturn's D-ring into its equatorial upper atmosphere. *Science* **362**, eaat2236 (2018).

37. S. Auer, Two high resolution velocity vector analyzers for cosmic dust particles. *Rev. Sci. Instrum.* **46**, 127–135 (1975).

38. J. R. Göller, E. Grün, Calibration of the Galileo/Ulysses dust detectors with different projectile materials and at varying impact angles. *Planet. Space Sci.* **37**, 1197–1206 (1989).

39. N. Altobelli, S. Kempf, M. Landgraf, R. Srama, V. Dikarev, H. Krüger, G. Moragas-Klostermeyer, E. Grün, Cassini between Venus and Earth: Detection of interstellar dust. *J. Geophys. Res.* **108**, 8032 (2003).

40. C. Tsitouras, A tenth order symplectic Runge-Kutta-Nyström method. *Celest. Mech. Dynam. Astron.* **74**, 223–230 (1999).

41. J. K. Campbell, J. D. Anderson, Gravity field of the Saturnian system from *Pioneer* and *Voyager* tracking data. *Astron. J.* **97**, 1485–1495 (1989).

42. C. D. Murray, S. F. Dermott, *Solar System Dynamics* (Cambridge Univ. Press, 1999).

43. E. Grün, H. A. Zook, M. Baguhl, A. Balogh, S. J. Bame, H. Fechtig, R. Forsyth, M. S. Hanner, M. Horanyi, J. Kissel, B.-A. Lindblad, D. Linkert, G. Linkert, I. Mann, J. A. M. McDonnel, G. E. Morfill, J. L. Phillips, C. Polanskey, G. Schwehm, N. Siddique, P. Staubach, J. Svestka, A. Taylor, Discovery of Jovian dust streams and interstellar grains by the Ulysses spacecraft. *Nature* **362**, 428–430 (1993).

44. V. J. Sterken, N. Altobelli, S. Kempf, G. Schwehm, R. Srama, E. Grün, The flow of Interstellar dust into the solar system. *Astron. Astrophys.* **538**, A102 (2012).

45. A. R. Poppe, The contribution of Centaur-emitted dust to the interplanetary dust distribution. *Mon. Not. R. Astron. Soc.* **490**, 2421–2429 (2019).

46. J.-C. Liou, H. A. Zook, S. F. Dermott, Kuiper Belt dust grains as a source of interplanetary dust particles. *Icarus* **124**, 429–440 (1996).

47. A. Moro-Martín, R. Malhotra, A study of the dynamics of dust from the Kuiper Belt: Spatial distribution and spectral energy distribution. *Astrophys. J.* **124**, 2305–2321 (2002).

48. M. Landgraf, J.-C. Liou, H. A. Zook, E. Grün, Origins of solar system dust beyond jupiter. *Astron. J.* **123**, 2857–2861 (2002).

49. G. Colombo, D. A. Lautman, I. I. Shapiro, The Earth's dust belt: Fact or fiction?: 3. Lunar ejecta. *J. Geophys. Res.* **71**, 5719–5731 (1966).

50. F. Spahn, N. Albers, M. Hörning, S. Kempf, A. V. Krivov, M. Makuch, J. Schmidt, M. Seiß, M. Sremˇević, E ring dust sources: Implications from Cassini's dust measurements. *Planet. Space Sci.* **54**, 1024–1032 (2006).

51. A. V. Krivov, M. Sremˇević, F. Spahn, V. V. Dikarev, K. V. Kholshevnikov, Impact-generated dust clouds around planetary satellites: Spherically symmetric case. *Planet. Space Sci.* **51**, 251–269 (2003).

52. J. N. Cuzzi, R. H. Durisen, Bombardment of planetary rings by meteoroids–General formulation and effects of Oort Cloud projectiles. *Icarus* **84**, 467–501 (1990).

53. T. McDonnell, N. McBride, S. F. Green, P. R. Ratcliff, D. J. Gardner, A. D. Griffiths, Near Earth Environment, in *Interplanetary Dust* (Springer, 2001), pp. 163–231.

54. A. Grigorieva, P. Thébault, P. Artymowicz, A. Brandeker, Survival of icy grains in debris discs. The role of photosputtering. *Astron. Astrophys.* **475**, 755–764 (2007).

55. D. T. Britt, G. J. Consolmagno, Stony meteorite porosities and densities: A review of the data through 2001. *Meteorit. Planet. Sci.* **38**, 1161–1180 (2003).

56. M. Fulle, V. Della Corte, A. Rotundi, P. Weissman, A. Juhasz, K. Szego, R. Sordini, M. Ferrari, S. Ivanovski, F. Lucarelli, M. Accolla, S. Merouane, V. Zakharov, E. Mazzotta Epifani, J. J. López-Moreno, G. Rodríguez, L. Colangeli, P. Palumbo, E. Grün, M. Hilchenbach, E. Bussoletti, F. Esposito, S. F. Green, P. L. Lamy, J. A. M. McDonnell, V. Mennella, A. Molina, R. Morales, F. Moreno, J. L. Ortiz, E. Palomba, R. Rodrigo, J. C. Zarnecki, M. Cosi, F. Giovane, B. Gustafson, M. L. Herranz, J. M. Jerónimo, M. R. Leese, A. C. López-Jiménez, N. Altobelli, Density and charge of pristine fluffy particles from comet 67P/Churyumov–Gerasimenko. *Astron. J.* **802**, L12 (2015).

57. D. Jewitt, J. Luu, Discovery of the candidate Kuiper belt object 1992 QB$_1$. *Nature* **362**, 730–732 (1993).

58. H. F. Levison, M. J. Duncan, From the Kuiper Belt to jupiter-family comets: The spatial distribution of ecliptic comets. *Icarus* **127**, 13–32 (1997).

Science Advances

Micrometeoroid infall onto Saturn's rings constrains their age to no more than a few hundred million years

Sascha Kempf, Nicolas Altobelli, Jrgen Schmidt, Jeffrey N. Cuzzi, Paul R. Estrada, and Ralf Srama

View the article online
https://www.science.org/doi/10.1126/sciadv.adf8537
Permissions
https://www.science.org/help/reprints-and-permissions

Use of this article is subject to the Terms of service